

Probing protoneutron star density profile from neutrino signals.

M. Baldo and V. Palmisano

INFN, Sezione di Catania

Via S. Sofia 64, I-95123, Catania, Italy

ABSTRACT

Supernovae of Type II is a phenomenon that occurs at the end of evolution of massive stars when the iron core of the star exceeds a mass limit. After collapse of the core under gravity the shock wave alone does not succeed in expelling the mass of the star and in this sense the role of neutrinos is the most important mechanism to do so. During the emission of neutrinos flavor conversion is possible, related the phenomenon of oscillations, which however depends directly on the particular density profile of the medium. In this paper we present results of numerical simulations of neutrino flavor conversion in protoneutron stars and after collapse. The probabilities of survival for a given flavor in a complete three-flavors framework is estimated through an algorithm which conserves unitarity to a high degree of accuracy. The sensitivity of the results to the different adopted models for the protoneutron star structure is examined in detail demonstrating how the neutrino signal could be used to check the validity of models.

PACS : 21.65.+f , 24.10.Cn , 26.60.+c , 03.75.Ss

I. INTRODUCTION

The solution of the solar neutrino "puzzle" [1, 2] has pointed out the relevance of the MSW mechanism [3] in the neutrino propagation through the dense medium of astrophysical objects. The mechanism is a consequence of the neutrino masses and the corresponding flavor mixing. If neutrino are emitted from the core of

a star, the initial flavor distribution can be distorted by the flavor conversion that can occur during the propagation outwards. On one hand this can be a complication in interpreting the possible neutrino signals, on the other hand the presence of conversion can be of great value in constraining the models of the astrophysical objects. The solar neutrino problem is a typical case where flavor conversion offers a solution of the puzzle and at the same time put serious constraints on the modeling of the internal structure of the star, which would not be easily accessible otherwise. All that has stimulated a large number of studies of neutrino propagation in more compact stars, like supernovae, protoneutron stars and neutron stars [4]. These astrophysical objects have a much larger central density and therefore neutrino flavor conversion can occur only in the outer part, where the density can decrease to values compatible with the MSW mechanism.

Of particular interest is the case of protoneutron stars, where the neutrinos of all three flavors can be considered in thermal equilibrium and thermally generated at the center of the stellar object. In principle the neutrino energy spectrum of each flavor is determined by the temperature at which they decouple from matter, i.e. the extension of the corresponding neutrino sphere. However, due to possible conversion through the MSW mechanism, the energy spectrum and each flavor fraction is modified after the propagation through the stellar medium. This modification depends crucially on the density profile, and therefore the neutrino signal can be used in principle to constraint the models of the protoneutron star structure and evolution. The effect of the shock wave on the neutrino signal has been analyzed in several papers [5, 6, 7], both as a function of time and in relation to neutrino mixing parameters. The dependence on the structure of the progenitor star has been analyzed in ref. [8], while the expected relic neutrinos characteristics have been studied in ref. [9].

However, to the authors knowledge, no systematic study of the relation between possible neutrino signals and protoneutron star structure have been carried out in the literature. In this work we present a detailed analysis of the neutrino propagation in the protoneutron star medium and we try to relate directly some characteristics of the neutrino signals to the star density profile, which, in principle, could be used to distinguish among different models or model parameters.

In this study we will neglect neutrino–neutrino interaction, which has been

recently shown [5] to be able to produce giant coherent flavor conversion. This coherent process can occur under particular conditions, and, to simplify the analysis, we do not consider this possibility in the paper.

II. GENERALITIES AND NUMERICAL METHOD.

It is customary to schematize the propagation of neutrinos outside the neutrino sphere as coherent and subject only to a single particle potential, i.e. only forward scattering is present [10]. The medium has then only the effect of shifting the neutrino masses locally at each point of the star. As it is well known, due to the dominance of electrons in the lepton content of the protoneutron star, this shift is flavor dependent and the neutrino mass spectrum is strongly altered. In fact, due to the electron dominance, electron neutrinos interact also through charged weak current, while the τ and μ neutrinos interact essentially through neutral weak current only. In the deep interior of the star the electron neutrino mass is shifted at much higher value than the neutrinos of the other two flavors. The mass spectrum is then formed by a singlet eigenstate, corresponding to pure electron neutrinos, and an eigenstate doublet below, involving the other two flavors. During the neutrino propagation outwards, the electron density decreases and the mass difference between the singlet and the doublet decreases, but to the extent that the mass difference stays large enough, the structure of the spectrum remains unaltered. Since, at least in the so called "direct hierarchy" scheme, the lowest neutrino mass in free space has a large electron flavor content, at a certain electron density the singlet eigenstate must cross the doublet and strong mixing can occur, i.e. neutrinos can jump among the different local (instantaneous) mass eigenstates, thus altering the neutrino populations among them. This is the essence of the MSW mechanism. According to the degree of adiabaticity of the process, some flavor conversion can occur, which determines the final flavor distribution. If the crossing is fast enough, the neutrinos in the initial electron flavor singlet eigenstate will jump in the lowest eigenstate, which will finally merge in the lowest neutrino mass in free space. The latter has a definite flavor content (mainly a mixture of electron and muon flavors). On the contrary, if the process is completely adiabatic, the neutrinos will remain in the same (higher) local mass

eigenstate, and finally they will propagate in the highest mass eigenstate in free space (mainly a mixture of τ and μ flavors).

From this simple considerations it is clear that the crucial parameter of the process is the adiabaticity and therefore the density profile, which fixes the local density slope, has a direct influence on the final neutrino signal. It is this connection between the density profile and the final mass and flavor populations that we want to exploit systematically in this paper.

In a simplified description where only two mass eigenstates are considered most of the calculations cannot be done analytically, and a fortiori in a more realistic description with all three flavors included only numerical simulations are possible. Following the standard treatment, the initial flavor distribution can be evolved by a 3×3 matrix. In the case of three neutrino the flavor eigenstate ν_e , ν_μ and ν_τ and mass eigenstate ν_1 , ν_2 and ν_3 are related through the linear relation

$$\begin{pmatrix} \nu_e \\ \nu_\mu \\ \nu_\tau \end{pmatrix} = \begin{pmatrix} U_{e1} & U_{e2} & U_{e3} \\ U_{\mu1} & U_{\mu2} & U_{\mu3} \\ U_{\tau1} & U_{\tau2} & U_{\tau3} \end{pmatrix} \begin{pmatrix} \nu_1 \\ \nu_2 \\ \nu_3 \end{pmatrix}. \quad (1)$$

In general, in the case of Dirac neutrinos the lepton mixing matrix U in eq. (1) depends on three mixing angles θ_{12} , θ_{13} and θ_{23} and one CP-violating phase δ , while in the case of Majorana neutrinos there are two additional, so-called Majorana phases. It is convenient to use the parametrization of the matrix U which coincides with the standard parametrization of the quark mixing matrix

$$U = \begin{pmatrix} c_{12}c_{13} & s_{12}c_{13} & s_{13}e^{-i\delta} \\ -s_{12}c_{23} - c_{12}s_{23}s_{13}e^{i\delta} & c_{12}c_{23} - s_{12}s_{23}s_{13}e^{i\delta} & s_{23}c_{13} \\ s_{12}s_{23} - c_{12}c_{23}s_{13}e^{i\delta} & -c_{12}s_{23} - s_{12}c_{23}s_{13}e^{i\delta} & c_{23}c_{13} \end{pmatrix} \quad (2)$$

where $c_{ij} = \cos\theta_{ij}$, $s_{ij} = \sin\theta_{ij}$. The probabilities of oscillations between various flavor states, unlike in the two-flavor case, are in general do not have a simple form. The evolution equation describing neutrino oscillations in matter is

$$i \frac{d}{dr} \begin{pmatrix} \nu_e \\ \nu_\mu \\ \nu_\tau \end{pmatrix} = \left[\frac{1}{2E} U \begin{pmatrix} m_1^2 & 0 & 0 \\ 0 & m_2^2 & 0 \\ 0 & 0 & m_3^2 \end{pmatrix} U^\dagger + \begin{pmatrix} V_{cc} & 0 & 0 \\ 0 & 0 & 0 \\ 0 & 0 & 0 \end{pmatrix} \right] \begin{pmatrix} \nu_e \\ \nu_\mu \\ \nu_\tau \end{pmatrix}. \quad (3)$$

Here U is the 3×3 flavor vacuum mixing matrix defined in Eq. (1) and $V_{cc}(r)$ is the matter-induced neutrino potential for unpolarized medium of zero total momentum defined in terms of electron number density $N_e(r)$ and Fermi constant G_F as

$$V_{cc}(r) = \sqrt{2} G_F N_e(r). \quad (4)$$

It is rather difficult to study this equation analytically, even in an adiabatic approximation. As we will see, the numerical treatment is necessary also because in some cases the density profile does not produce a real MSW resonance, but rather a “modulation” of the flavor populations, which can be hardly treated analytically. This requires a quite stable numerical algorithm in solving iteratively eq. (3). We used a method, based on the Hamilton-Caley theorem, which guarantees the fulfillment of unitarity to a very high degree of accuracy and it is therefore suitable for calculations which extend for large time and long distances. Typically the calculations were performed from the center to the stars up to 10^7 kilometers.

Contrary to other methods used to solve the evolution equations of the neutrino states by means of techniques like Runge-Kutta or similar our numerical algorithm using the Hamilton-Caley’s theorem assures unitarity of the evolution operator to a very high degree of accuracy. If the wave function of the flavor triplet of a neutrino is written as a three components vector $\psi_\nu \equiv (\nu_e, \nu_\mu, \nu_\tau)^T$ the flavor evolutions is completely determined by the Schrödinger equation in the compact form

$$i \frac{d}{dr} \psi_\nu(r) = H \psi_\nu(r) \quad (5)$$

where the matrix H is the Hamiltonian operator. The code obtain $\psi_\nu(l + \delta l)$ from $\psi_\nu(l)$ using an iterative procedure step by step:

$$\psi_\nu(l + \delta l) \simeq e^{-iH\delta l} \psi_\nu(l) \quad (6)$$

preserving the unitarity of ψ_ν automatically and becoming exact if H is independent of spatial coordinate. Therefore the step sizes employed in numerical codes are not restricted by the size of H but are restricted by the rate of change of H . In this algorithm the Hamilton-Caley's theorem is used to calculate step by step the exponential operator in the eq. (6) to determinate the evolution of ψ_ν both in the simple two flavors framework and in the standard three flavor framework.

III. NEUTRINO SIGNALS AND THE PROTONEUTRON STAR STRUCTURE.

Numerical simulations of the collapse and evolution of supernovae up to the stage of protoneutron star is quite difficult and affected by many uncertainties. For these reason simulations up to few tens of seconds after collapse are quite rare. The reference simulations are those of the Livermore group [11], which are often used in the literature for different types of analysis. These simulations include also the shock wave front. Phenomenological models are also used for qualitative considerations [6].

At the protoneutron star stage of the evolution neutrinos are essentially thermally produced. If all three flavors had the same temperature at the moment of decoupling from matter, i.e. the neutrino sphere is independent of flavor, then all three flavors had the same fraction of 1/3 and the same energy spectrum. Any possible conversion mechanism would not affect such a population distribution and no characteristic neutrino signal could be present. It is therefore essential to specify the initial temperature and chemical potential for each flavor in the core of the star. For definiteness we will follow ref. [12], but with the possibility of slightly modify the parameters to check the sensitivity of the results on their specific values. Each flavor population is described by a Fermi distribution

$$f_\nu(E) \equiv \frac{1}{F_2(\eta_\nu)} \frac{1}{T_\nu^3} \frac{E^2}{\exp(E/T_\nu - \eta_\nu) + 1}, \quad (7)$$

where η_ν is the degeneracy parameter, T_ν is the neutrino temperature and

$$F_k(\eta) \equiv \int_0^\infty \frac{x^k dx}{\exp(x - \eta) + 1} \quad (8)$$

is the Fermi integral with rank $k = 2$.

The values of the degeneracy parameters are taken $\eta_{\nu_e} = \eta_{\nu_\mu} = \eta_{\nu_\tau} = 3$ and neutrino temperatures are taken $T_{\nu_e} \simeq 2.76$ MeV and $T_{\nu_\mu} = T_{\nu_\tau} \simeq 6.26$ MeV. The normalization factors $F_2(\eta_\nu)$ specify also the total content of each flavor. Once the initial conditions are fixed, one has to define the parameters of the flavor mixing 3×3 matrix. Presently the only parameter that remain uncertain is the so-called θ_{13} mixing angle, while for all the others, standard established values can be used [4]. We choose the value $\sin^2 \theta_{13} = 10^{-4}$.

Since the density profile changes with time also the final neutrino signal is expected to change with time. For illustration, at the fixed time of $t = 4$ s and for the energy $E = 3$ MeV the flavor survival probabilities are reported in Fig. 1 as a function of the distance from the core of the star up to radius of 10^7 kilometers, where the influence of matter is surely not relevant. For this reason the probabilities or transition probabilities are usually rapidly oscillating in the final part of the propagation. We have then followed an averaging procedure over many oscillation period to establish the final average value of each flavor content. This is justified by the wide region where neutrino are actually emitted, which introduces a random phase. In any case, one can easily recognize the place where the MSW resonances occur.

This actually corresponds to the *higher* resonance, i.e. the place where the initial highest mass eigenvalue crosses the first one below.

In each row is reported the survival probability of each flavor (along the diagonal) and the contribution to each flavor coming from the other two flavors (off diagonal panels). In other words each panels contains the evolution of the flavor conversion probabilities along the neutrino path. At each radial distance r the sum of the values reported in a given row gives the total survival probability of each flavor. It has to be noticed the relevance of the “re-population” of e.g. the electron flavor by the other two flavors, without which the electron flavor content would drop to zero. Another example with different values of energy and fixed time is in Fig. 2. Of course the density profile changes during the neutrino propagation but the main conversion processes occur in a time interval short enough that the density profile can be considered fixed. In this sense the nominal value of time $t(s)$ must be taken just as a nominal value labeling the particular case considered.

From figures 1 and 2 it is apparent the interplay of the MSW conversion process and the non-resonant modulation due to the density profile. This is mainly due to the fact that the MSW resonance width is quite wide, and some degree of flavor conversion can occur even if the resonance density is not strictly crossed. The final signal depends in a complex way on the density profile. This also indicates the need of numerical calculations. It has to be stressed that the density at which the MSW resonance is expected to occur is quite low with respect to the typical nuclear density and in this density region matter is dominated by electrons, positrons and photons. However, the overall density profile depends also indirectly on the nuclear Equation of State (EOS), since the EOS is one of the main physical ingredient which determines the evolution and structure of the protoneutron star, and thus the density profile even in its outer part.

We have repeated these calculations at different times and different neutrino energies. The final neutrino energy spectrum of each flavor can be then extracted at different protoneutron star evolution time. This can be obtained by multiplying the initial Fermi distributions by the survival probability. In Fig. 3 is reported the fraction of electron neutrino for two different times as a function of neutrino energy. It is clear that in these cases the electron neutrino fraction is only slightly modulated as a function of time. Also the initial spectrum is affected by the propagation through the protoneutron star matter, however the final spectrum is expected to change only slightly at different times.

Indeed the spectrum is reported in Fig. (4) at the two different times in comparison with the initial one. It has to be noticed the strong distortion of the initial spectrum, due to the conversion process, but this distortion depends little on time. Of course the overall normalization depends on the total neutrino flux, but the considered properties, i.e. the electron neutrino fraction and the corresponding spectrum, do not depend on the value of the flux.

To see the sensitivity of these results on the density profile we have repeated the calculations by changing artificially the density profile of the protoneutron stars. To this purpose we have followed the profile parametrization introduced in ref. [6], according to which the density profile can be effectively approximated for post-bounce times $t \lesssim 1$ s as

$$\frac{\rho_0(r)}{\text{g/cm}^3} \approx 10^{14} \left(\frac{r}{\text{Km}} \right)^{-\alpha} \quad (9)$$

and for post-bounce time $t \gtrsim 1$ s as

$$\rho(r) = \rho_0(r) \cdot \begin{cases} \xi \cdot f(r) & , \quad r \leq r_S \\ 1 & , \quad r \geq r_S \end{cases} \quad (10)$$

where $\xi \simeq 10$ and the function $f(r)$ parametrizes the rarefaction zone above the shock front. The parametrization for $f(r)$ is taken

$$\ln f(r) = [0.28 - 0.69 \ln(r_S/\text{Km})] \cdot [\arcsin(1 - r/r_S)]^{1.1}. \quad (11)$$

In eq. (10) and eq. (11) it is assumed a slightly accelerating shock-front position x_S ,

$$r_S(t) = r_S^0 + v_S t + \frac{1}{2} a_S t^2 \quad (12)$$

with parameters fixed by

$$\begin{aligned} x_S &\simeq -4.6 \times 10^3 \text{km} , \\ v_S &\simeq 11.3 \times 10^3 \text{km/s} , \\ a_S &\simeq 0.2 \times 10^3 \text{km/s}^2 , \end{aligned} \quad (13)$$

The value of the parameter $\alpha = 2.4$ corresponds to the parametrization which reproduce closely the simulations of ref. [11], and this is the value used in the calculations reported above. We then varied the value of α to obtain a steeper or a more shallow density profile, which should possibly reflect different model simulations of the proton-neutron star dynamics. This is illustrated in Fig. 5 , where the density profiles for different values of α are compared at fixed times.

The modification of the profile has a direct effect on the neutrino fraction as shown in Fig. 6 for the case of $\alpha = 2.1$. At the lower energy, below about 15 MeV, the electron neutrino fraction presents a sharp drop at an early time evolution of the protoneutron star. This means that the electron neutrino energy spectrum should be drastically suppressed in the low energy part. At a later stage the energy spectrum should change again. The final spectra at the two different

times, in comparison with the initial Fermi-Dirac spectrum, for electron neutrinos are reported in Fig. 7. Also in this case the final spectrum is strongly distorted by the conversion process which occurs during the neutrino propagation in the protoneutron star matter, but what is relevant is that the distortion depends now more clearly on time. The increase of the high energy tail is due to the conversion of μ and τ neutrinos in electron neutrinos. Modification of the initial Fermi-Dirac distribution can also occur due to energy dependence of the neutrino transparency [13], but the type of dynamical evolution of the spectrum reported in Fig. 7 should be a distinct feature of a shallow density profile, also independent of the total neutrino flux, which also depends on time. Comparison between Figs. 3,4 and Figs. 6,7 shows the sensitivity on the density profile of the protoneutron stars during its evolution.

The reason for such a behavior is directly linked to the higher degree of adiabaticity of the MSW mechanism, in the wider sense discussed above. In fact, increasing the value of α to 2.7 both electron neutrino fraction and spectrum become almost independent of time, see Figs. 8,9.

We have also tested the dependence of the results on the assumed values of the neutrino temperatures. Decreasing the temperature differences all the considered effects decrease, which indicate the possibility of measuring the original neutrino temperatures.

IV. CONCLUSIONS.

In this paper we have presented evidence of possible neutrino signals from protoneutron stars based on the flavor conversion processes which can occur inside the star and which are sensitive to the density profile of these astrophysical compact objects. Generally speaking a more shallow density profile would produce a percentage of electron neutrino strongly suppressed at low energy, approximately below 15 MeV, few second after collapse. This suppression should disappear after 10-20 seconds. Correspondingly, the electron neutrino spectrum should show a characteristic time dependence.

Of course, all these signals require an appreciable number of events in the detectors, and only with the next generation of neutrinos detectors one can hope

to have indications of the signals studied in the present paper.

- [1] K. Eguchi et al. Phys. Rev. Lett. **90**, 021802 (2003).
- [2] W.C. Haxton, Phys. Rev. Lett. **57**, 1271 (1986).
- [3] S.P. Mikheyev and A. Yu Smirnov, Nuovo Cimento **9C**, 17 (1986) ; L. Wolfenstein, Phys. Rev. **D 16**, 2369 (1988).
- [4] A.B. Balantekin and W.C. Haxton, arXiv:nucl-th/9903038.
- [5] H. Duan, G.M. Fuller, J. Carlson and Y.-Z. Qian, Phys. Rev. Lett. **97**, 241101 (2006).
- [6] G.L. Fogli, E. Lisi, A. Mirizzi and D. Montanino, Phys. Rev. D **68**, 033005 (2003).
- [7] Y.-Z. Qian and G.M. Fuller, Phys. Rev. D **51**, 1479 - 1494 (1995).
- [8] K. Takahashi, K. Sato, A. Burrows and T.A. Thompson, Phys. Rev. **D 68**D68 , 113009 (2003).
- [9] C. Volpe and J. Welzel, arXiv:0711.3237 [astro-ph].
- [10] A. Friedland and C. Lunardini, Phys. Rev. **D 68**, 013007 (2003).
- [11] J.R. Wilson, R. Mayle, S. Woosely and T. Weaver, N.Y. Acad. Sci. **470** 267 (1986).
- [12] H. Duan, G.M. Fuller, J. Carlson and Y.-Z. Qian, Phys. Rev. **D74** 105014 (2006), arXiv:astro-ph/0606616.
- [13] M.T. Keh, G.G. Raffelt and H.-T. Janka, ApJ. **590** 971 (2003).

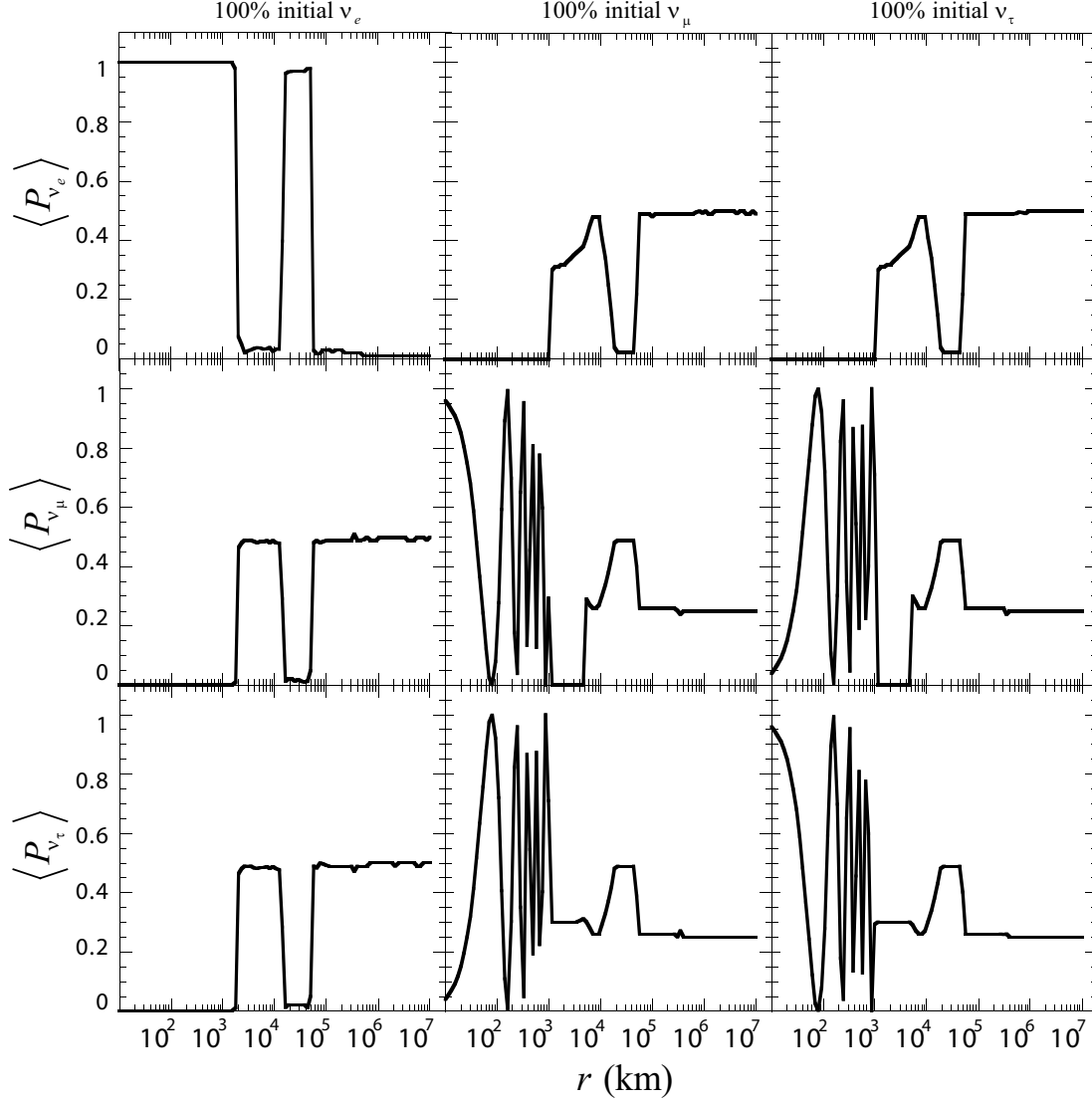


FIG. 1: Survival probabilities and transition probabilities for different flavors along neutrino path inside the protoneutron star matter. The energy of neutrinos is 3 MeV and the time after bounce is $t = 4$ s. The density profile is characterized by the parameter $\alpha = 2.1$, see the text for detail

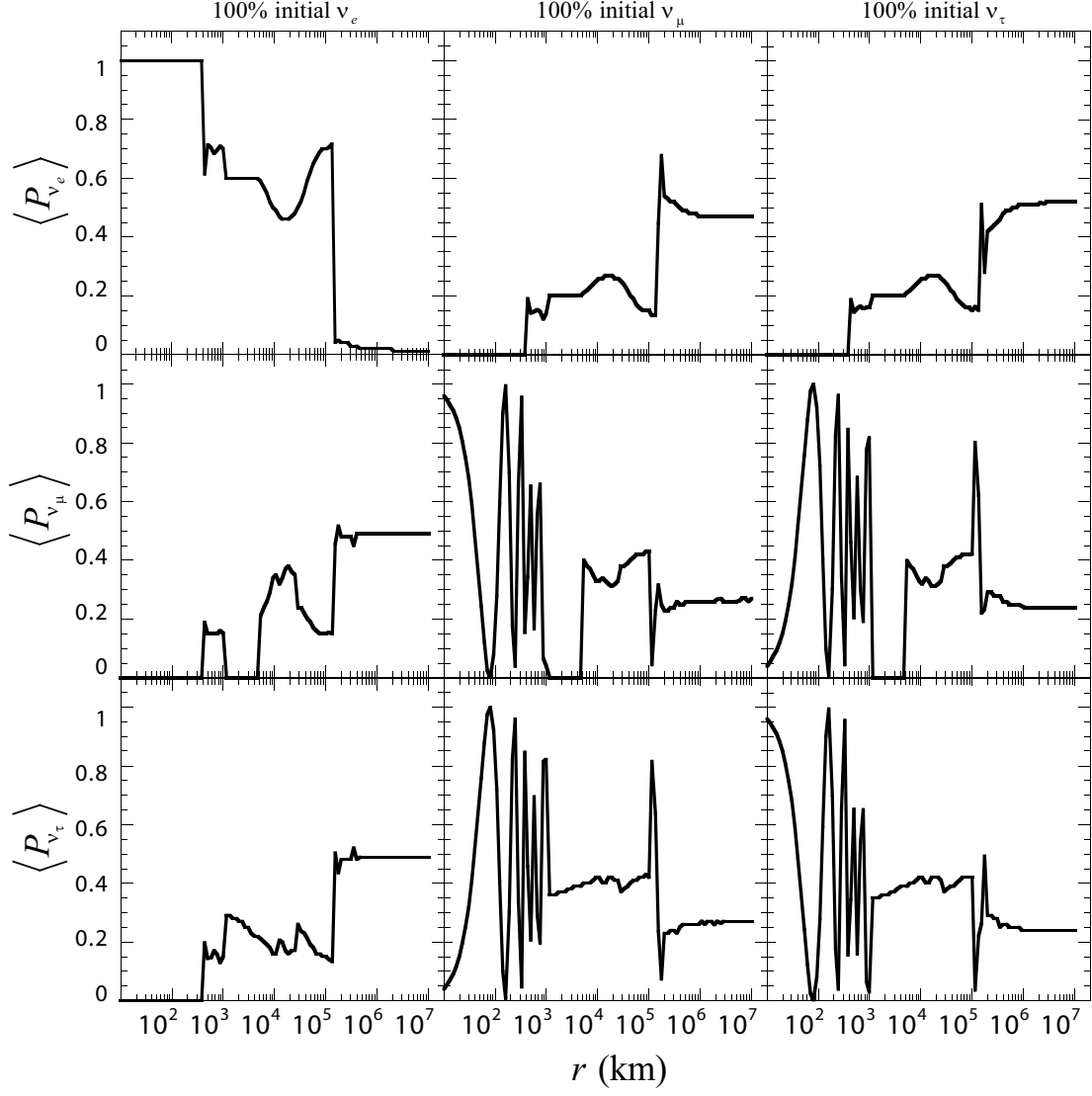


FIG. 2: The same as in Fig. 1 but at the different time $t = 12$ s.

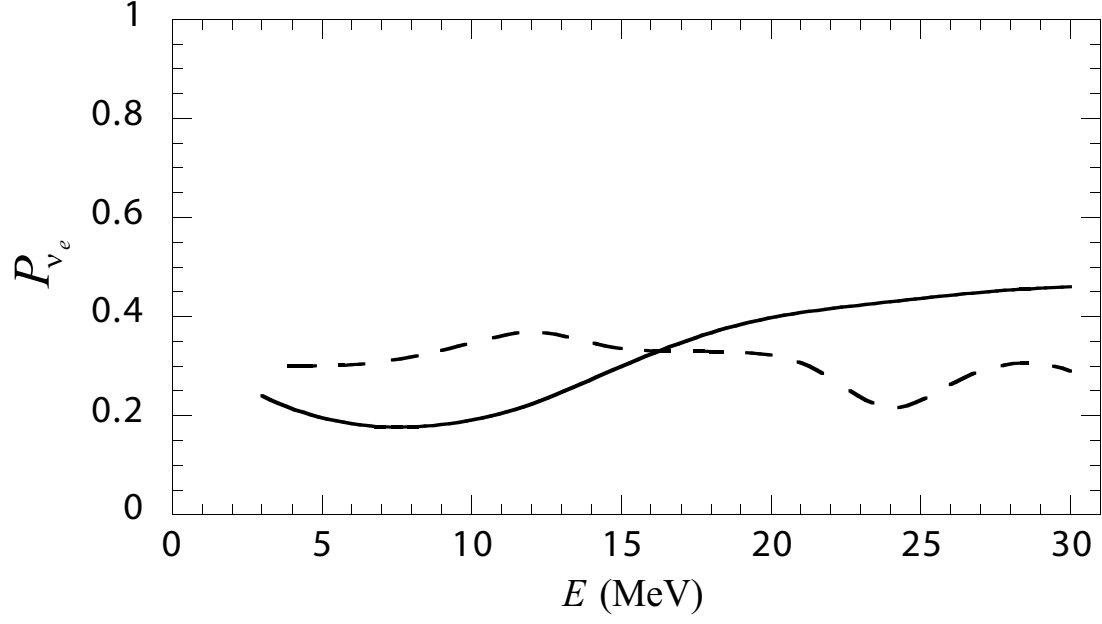


FIG. 3: Fraction of electron neutrinos as a function of energy at $t = 4$ s (full line) and $t = 27$ s (dashed line) after bounce. The parameter of the profiles has been fixed at $\alpha = 2.4$.

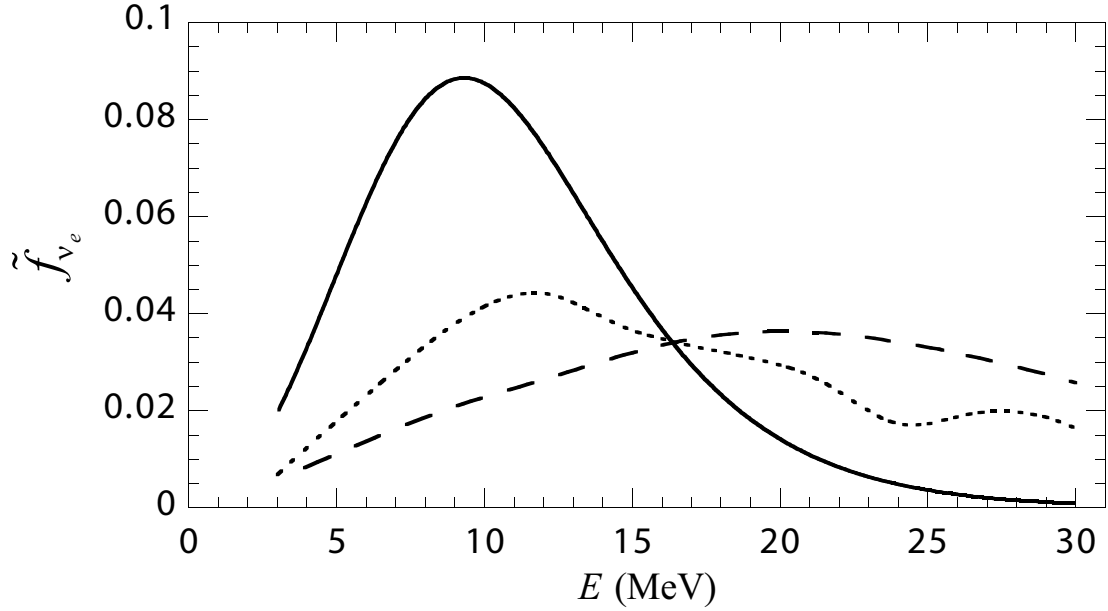


FIG. 4: electron neutrino spectrum corresponding to the case of Fig. 3. The full line is the initial Fermi-Dirac spectrum, the dashed line is the spectrum at $t = 4$ s and the dotted line at $t = 27$ s.

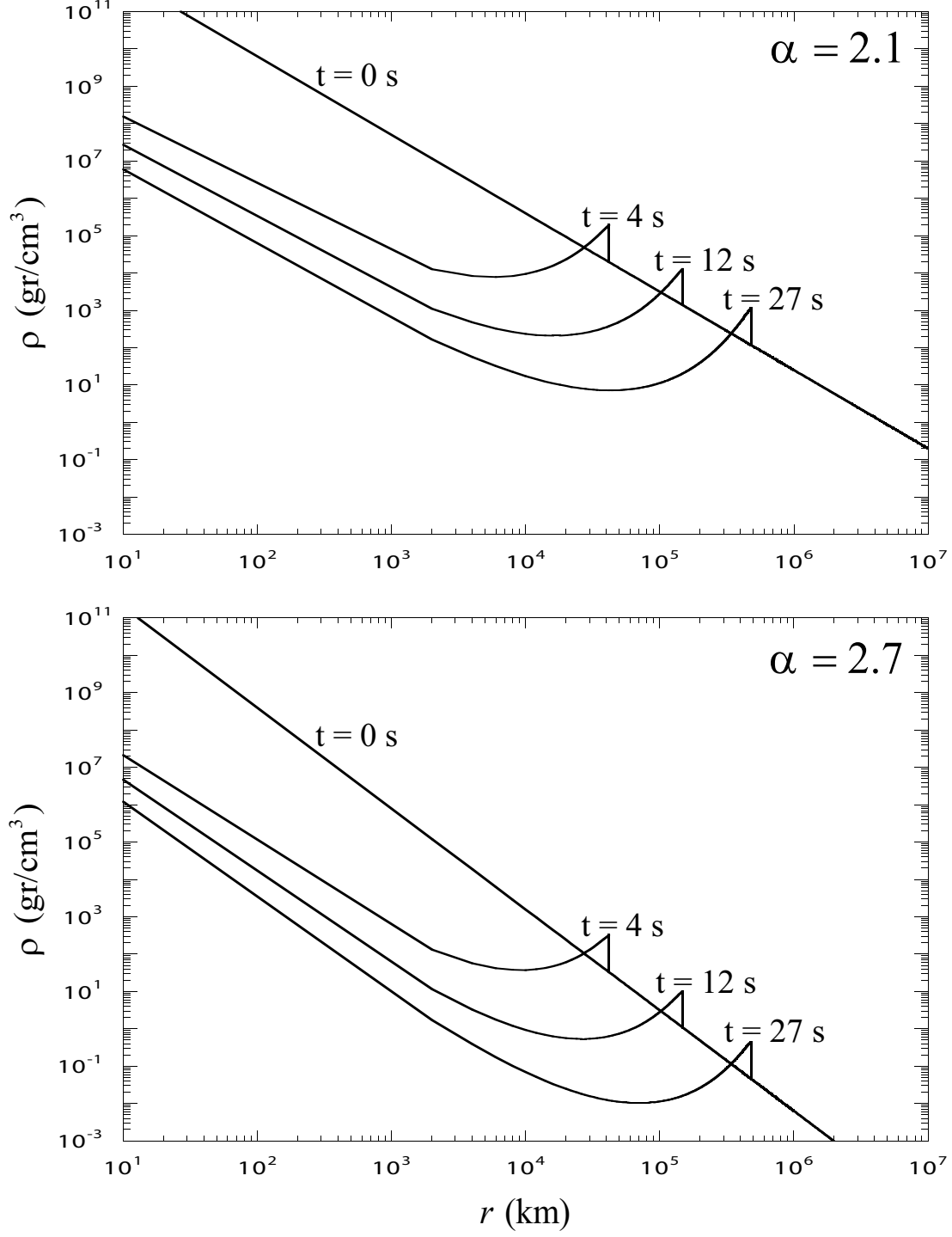


FIG. 5: Density profiles at different times after bounce corresponding to $\alpha = 2.1$ (left) and to $\alpha = 2.7$ (right).

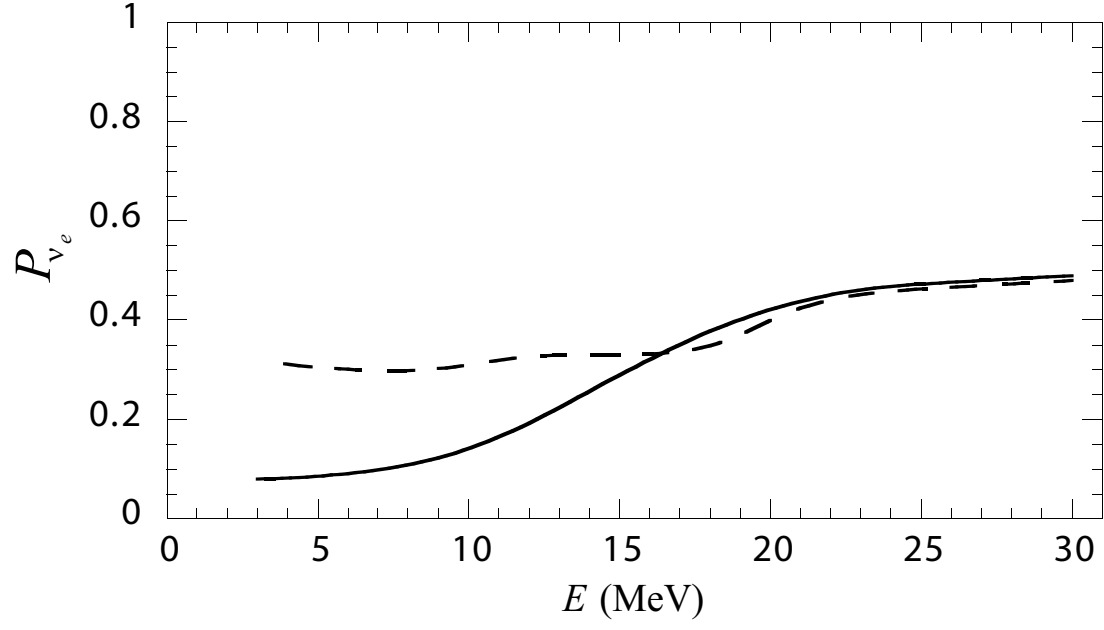


FIG. 6: The same as in Fig. 3 but for $\alpha = 2.1$.

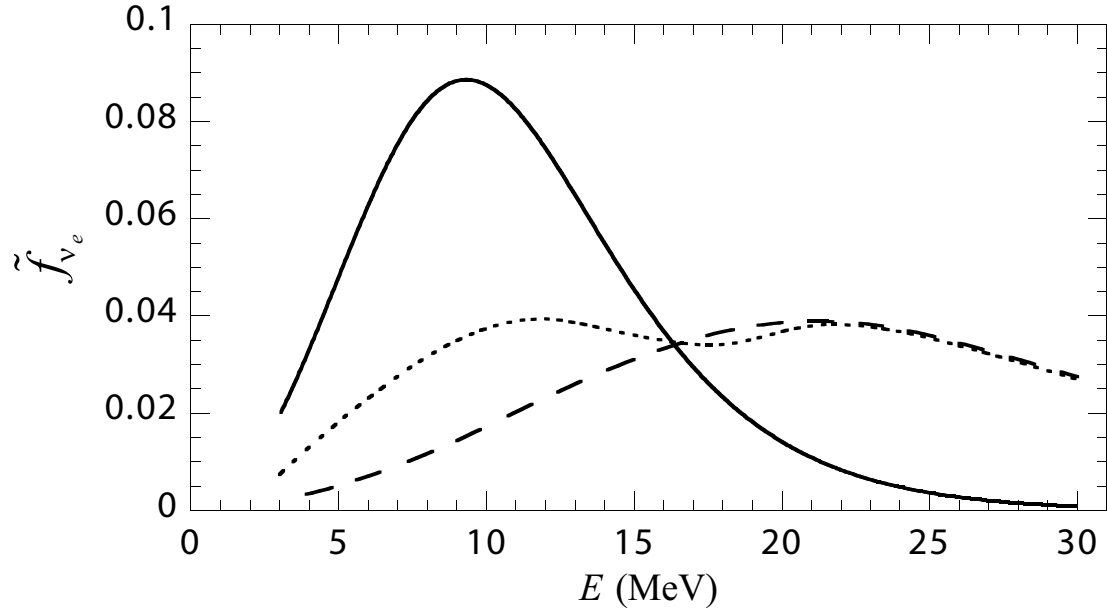


FIG. 7: The same as in Fig. 4 but for $\alpha = 2.1$.

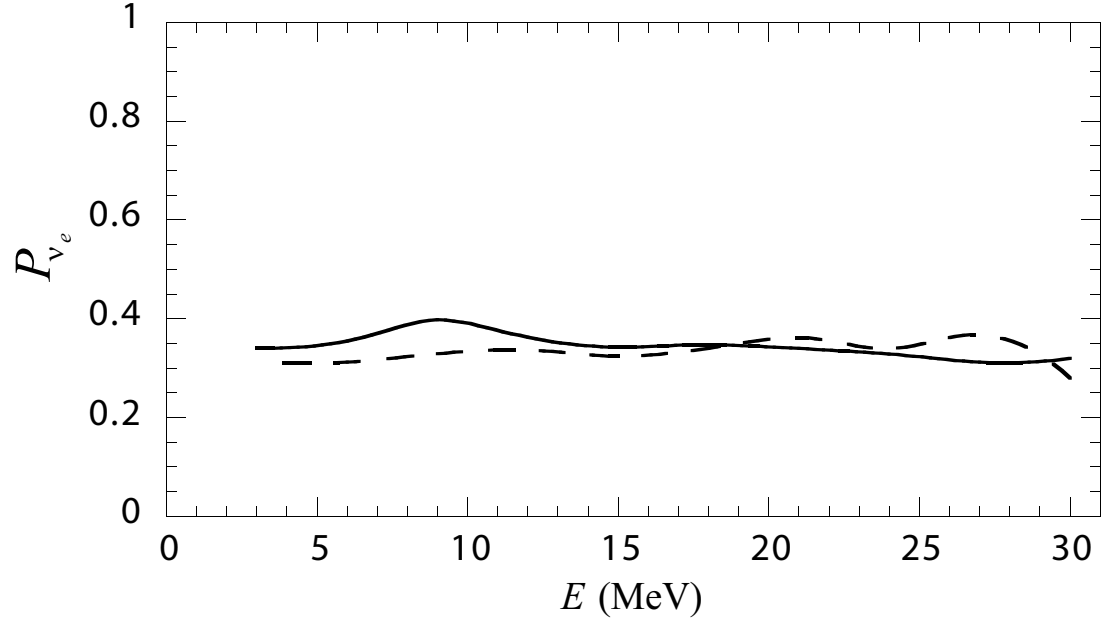


FIG. 8: The same as in Fig. 3 but for $\alpha = 2.7$.

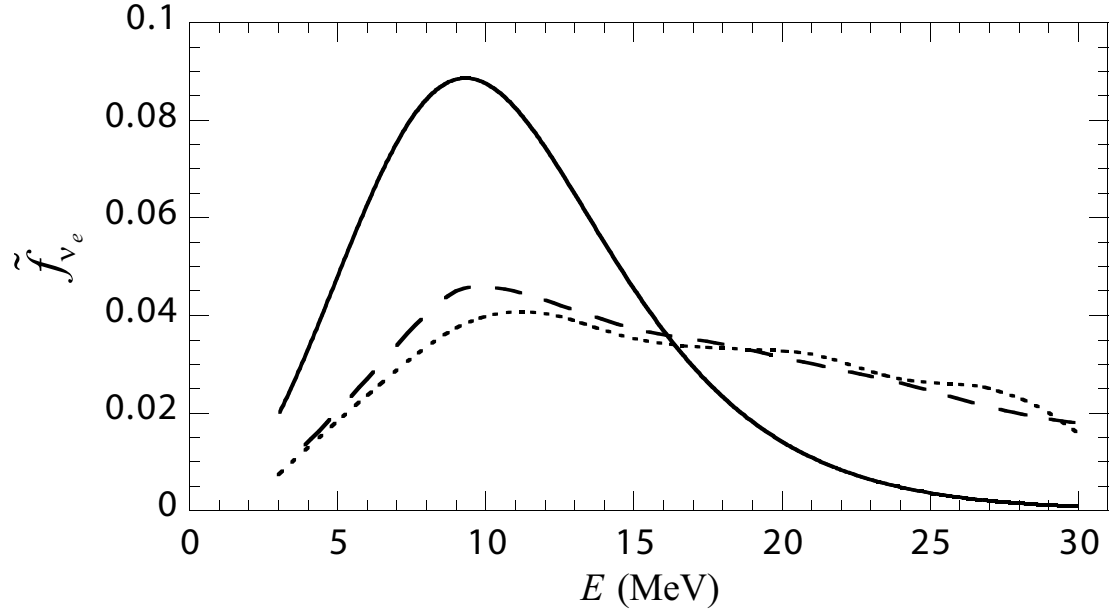


FIG. 9: The same as in Fig. 4 but for $\alpha = 2.7$.